ARTICLE

Effects of Current upon Electrochemical Catalytic Reforming of Anisole

Jia-xing Xiong, Tao Kan, Xing-long Li, Tong-qi Ye, Quan-xin Li*

Department of Chemical Physics, Lab of Biomass Clean Energy, University of Science and Technology of China, Hefei 230026, China

(Dated: Received on June 17, 2010; Accepted on September 6, 2010)

The reforming of anisole (as model compound of bio-oil) was performed over the NiCuZn-Al_2O_3 catalyst, using a recently-developed electrochemical catalytic reforming (ECR). The influence of the current on the anisole reforming in the ECR process has been investigated. It was observed that anisole reforming was significantly enhanced by the current approached over the catalyst in the electrochemical catalytic process, which was due to the non-uniform temperature distribution in the catalytic bed and the role of the thermal electrons originating from the electrified wire. The maximum hydrogen yield of 88.7% with a carbon conversion of 98.3% was obtained through the ECR reforming of anisole at 700 °C and 4 A. X-ray diffraction was employed to characterize catalyst features and their alterations in the anisole reforming. The apparent activation energy for the anisole reforming is calculated as 99.54 kJ/mol, which is higher than ethanol, acetic acid, and light fraction of bio-oil. It should owe to different physical and chemical properties and reforming mechanism for different hydrocarbons.

Key words: Hydrogen, Anisole, NiCuZn-Al_2O_3, Electrochemical catalytic reforming

I. INTRODUCTION

The increasing dependence on fossil fuels has caused serious environmental problems related to air pollution, acid rain, and climate changes, leading to the urgent utilization of renewable clean energy sources as an alternative in recent years. Concerning about its high heat value (120.7 kJ/g) and none environmental pollutants emission, hydrogen is recognized as a clean fuel and ideal energy carrier. In particular, its production is attractive for fuel cell applications [1, 2], which are considered to have the potential to be a clean energy source for automobile. Currently, main processes for producing commercial hydrogen are catalytic steam reforming of natural gas and oil-derived naphtha, partial oxidation of heavy oils, gasification of coal as well as electrolysis of water [1, 3]. In view of growing environmental concerns such as global warming and the depletion of fossil fuel, great efforts are being dedicated to the utilization of renewable energy sources. Biomass is a rich, environmental friendly, renewable and globally available resource, which can be used as an alternative feedstock for hydrogen production [4, 5].

There are different routes proposed for conversion of biomass into hydrogen-rich gas or hydrogen, mainly including thermochemical and bio-chemical conversion [6]. For the production of hydrogen by thermochemical conversion, several technologies such as biomass gasification and biomass catalytic pyrolysis followed by reforming have been widely explored [7−11]. Steam reforming of pyrolysis oil (*i.e.*, bio-oil produced via the process of biomass pyrolysis) appears to be an attractive technology for the production of hydrogen. Biomass fast pyrolysis technology is a thermal decomposition process that converts biomass into organic liquids by fast heating the biomass in the absence of air at around 400−600 °C with yields as high as 75%−80% (including water) [12−15]. In the view of economy and environment, steam reforming of pyrolysis oil (bio-oil) is one of the promising routes of hydrogen production from renewable sources.

Although substantial research on the steam reforming of hydrocarbons (*e.g.*, CH_4) and single oxygenated organic compound (*e.g.*, methanol, ethanol, acetic acid *etc.*) has been carried out and well-reviewed in the past [2, 16, 17], two main problems, exorbitant reforming temperature and the catalyst deactivation, still exist in the hydrogen production from bio-oil [18, 19]. Compared with the reforming process of simple model compounds (*e.g.*, ethanol, acetic acid *etc.*), the bio-oil reforming seems quite different, at least in following three respects. Firstly, an efficient conversion reforming temperature of bio-oil for a given catalyst, generally, is much higher than those model compounds. For example, an almost complete conversion of ethanol (about 98%) [17] and a 42% conversion of acetic acid [16] can be obtained at 400 °C using the 18% NiO/Al_2O_3 catalyst. However, the conversion of light fraction of bio-oil using the same catalyst was very low (about 14.7%) at

*Author to whom correspondence should be addressed. E-mail: liqx@ustc.edu.cn

400 °C and only reached 65.4% even at 600 °C [20]. Higher operating temperature for the bio-oil reforming may be attributed to the fact that the bio-oil contains large amount of lower reforming active compounds such as phenolics and ketones *etc.* Secondly, the catalyst inactivity and carbon deposition in the bio-oil reforming, generally, is much more serious than those oxygenated model compounds [16−20]. Thirdly, the reaction channels in the bio-oil reforming should be much more complex than the single organic compounds because the bio-oil contains multi-types organic compounds. To maximize the carbon efficiency of bio-oil, anisole was taken as a model compound for methoxy functional groups in lignin-derived fraction [21−25] to investigate the reforming mechanism of phenolics.

In the previous work, our lab has developed a novel electrochemical catalytic reforming (ECR) method [16−20], in which an electrified Ni-Cr wire was used for heating the catalyst and synchronously providing thermal electrons onto the catalyst bed during the bio-oil reforming. The catalytic steam reforming of the volatile fraction of the bio-oil and its model compounds (ethanol, acetic acid) has been investigated utilizing the ECR method [16−20]. Present work is focused on the reforming of anisole (as one of the model compounds of bio-oil) via the recently-developed ECR approach over the NiCuZn-Al_2O_3 catalyst. The differences and mechanism for the reforming of anisole, ethanol, acetic acid, and light fraction of bio-oil was addressed based on present investigation.

II. EXPERIMENTS

A. Catalyst preparation

The NiCuZn-Al_2O_3 catalyst filled in the downstream reforming fixed bed was prepared by the co-precipitation method. The precipitate containing elements of Ni, Cu, Zn, and Al was prepared at a constant pH (9.0±0.2) using respective metal nitrates as precursors at a molar ratio of 2:1:1:4 and a mixture of NaOH (1 mol/L) and Na_2CO_3 (1 mol/L) as precipitants. The precipitate was extracted by suction filtration and washed to neutral. After being dried at 120 °C for 8 h, it was heated at a rate of 2 °C/min in air to 450 °C and calcined for 5 h to obtain the desired catalyst. Finally, the catalyst is crushed to an average diameter of 0.18−0.50 mm to install in the quartz tube reactor. All the catalyst samples in our tests were reduced *in situ* in hydrogen flow of 50 mL/min at 650 °C for 1 h at the beginning of experiment.

B. Reaction system

As shown in Fig.1, the anisole steam reforming experiments were carried out in the continuous flow systems,

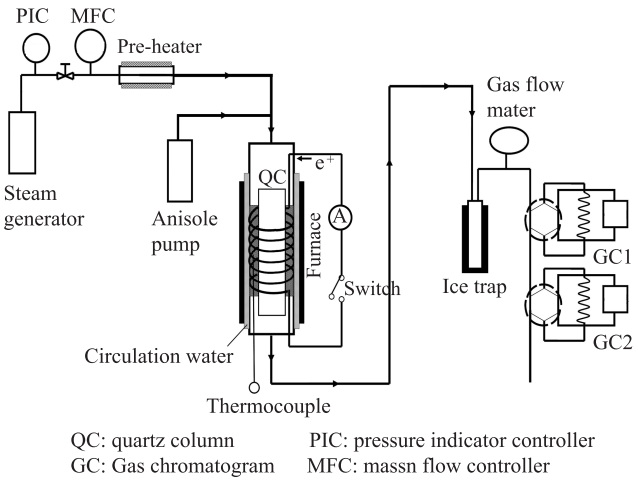

FIG. 1 Schematic setup of the fixed-bed flow reaction system for anisole in ECR and CSR mode. ECR mode: the catalyst was uniformly embedded around the annular Ni-Cr wire, which passed through an ac electronic current for heating the catalyst and synchronously providing the electrons onto the catalyst. CSR mode: the current was shut off and the reactor was homogeneously heated by an outside furnace.

using a quartz fixed-bed reactor under atmospheric pressure. Anisole was fed into the reactors using the micro-injection pump (Model: TS2-60, Baoding Longer Precision Pump). Steam from a steam-generator was simultaneously fed into the reactors for adjusting the S/C ratio (mole ratio of steam to carbon in anisole fed). The steam fed rate was controlled by the mass flow controller. Temperature and its distribution were measured by the thermocouple inserted into the catalyst beds. We performed the reforming experiments with following two modes, *i.e.*, the conventional steam reforming (CSR) mode and the ECR mode. For the ECR mode, an annular Ni-Cr wire, which passed through a given ac electronic current, entwined around a quartz column for heating the catalyst and synchronously providing the electrons onto the catalyst, and installed in the center of the reactor. The catalyst was uniformly embedded around the Ni-Cr wire. To maintain a certain reforming temperature, the catalyst bed was simultaneously heated by an outside furnace for compensation. For the CSR mode, ac current was shut off and the catalyst bed was homogeneously heated by the outside furnace.

The final gaseous products of H_2, CO, CO_2, and CH_4 were measured by on-line gas chromatograph (Model: SP6890, TDX-01) with thermal conductivity detector (TCD), using ultra-high purity argon (99.999%) as carrier gas. The performance of anisole catalytic steam reforming was studied by measuring the carbon conversion of anisole to gases $[C]_{conv}$, the conversion of anisole $[A]_{conv}$, the hydrogen yield Y_{H_2}, and distribution of product gases. The carbon conversion is calculated according to Eq.(1) and expressed as the percentage of

DOI:10.1088/1674-0068/23/06/693-700

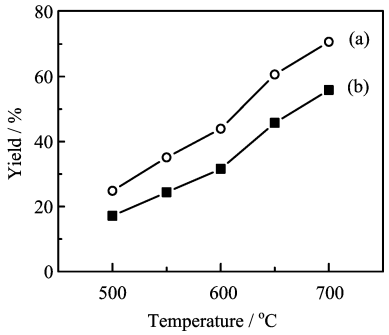

FIG. 2 Effect of temperature on carbon conversion (a) and H_2 yield (b) of anisole steam reforming over NiCuZn-Al_2O_3 catalyst. Conditions: T=500−700 °C, f(anisole fed rate)=5.97 g/h, S/C=8, GHSV=2380 h^{-1}, P=101 kPa.

carbon from the fed anisole to the final gaseous products (*i.e.*, CO, CO_2, and CH_4).

$$[\mathrm{C}]_{\mathrm{conv}} = \frac{x_{\mathrm{gC}}}{x_{\mathrm{fC}}} \times 100\% \quad (1)$$

$$[\mathrm{A}]_{\mathrm{conv}} = \frac{x_{\mathrm{inA}} - x_{\mathrm{outA}}}{x_{\mathrm{inA}}} \times 100\% \quad (2)$$

$$Y_{\mathrm{H_2}} = \frac{x_{\mathrm{H_2o}}}{x_{\mathrm{H_2s}}} \times 100\% \quad (3)$$

$$S_{\mathrm{P}} = \frac{x_{\mathrm{P}}}{\chi(x_{\mathrm{inA}} - x_{\mathrm{outA}})} \times 100\% \quad (4)$$

$$S_{\mathrm{H_2}} = \frac{x_{\mathrm{H_2}}}{4(x_{\mathrm{inA}} - x_{\mathrm{outA}})} \times 100\% \quad (5)$$

$[\mathrm{A}]_{\mathrm{conv}}$, $Y_{\mathrm{H_2}}$, the products selectivity (CO, CH_4, CO_2, *etc.*) denoted as S_{P}, and hydrogen selectivity as $S_{\mathrm{H_2}}$ are calculated according to Eqs.(2)−(5). x_{gC} is moles of carbon in the gaseous products, x_{fC} is moles of carbon in the feed, x_{inA} is moles of anisole in, x_{outA} is moles of anisole out, $x_{\mathrm{H_2}}$ is moles of H_2, $x_{\mathrm{H_2o}}$ is moles of H_2 obtained, $x_{\mathrm{H_2s}}$ is moles of H_2 in stoichiometric potential, x_{P} is moles of the reaction products, and χ are the stoichiometry factors, P stands for the reaction products. All tests were repeated three times. The reported data were the mean values of the repeated trials.

III. RESULTS AND DISCUSSION

A. Effect of current on catalytic steam reforming of anisole

Generally, the performance of the anisole reforming using the CSR method is mainly controlled by the reforming temperature for a given catalyst. As shown in Fig.2, increasing temperature remarkably increased both the carbon conversion and the hydrogen yield. The hydrogen yield was about 17.1% at 500 °C and increased to 55.8% at 700 °C in the CSR mode. This is due to that the anisole reforming is an endothermic reaction, and increasing temperature will increase the reforming reaction rate. On the other hand, it was also

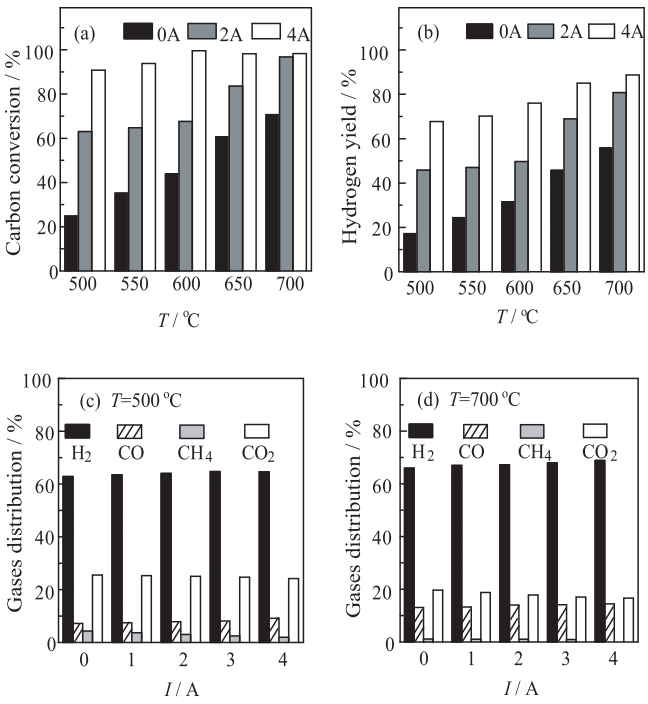

FIG. 3 Effect of current on the carbon conversion (a) and H_2 yield (b) of anisole steam reforming over NiCuZn-Al_2O_3 catalyst. (c) and (d) Effect of current on the distribution of gaseous products of anisole steam reforming over NiCuZn-Al_2O_3 catalyst. Conditions: f(anisole fed rate)=5.97 g/h, S/C=8, GHSV=2380 h^{-1}, P=101 kPa.

observed that the behavior of the anisole reforming was very sensitive to the current applied through the catalyst, which was described as the ECR. To investigate the features of the electrochemical catalytic reforming, the anisole reforming and its decomposition were performed under different current; meanwhile other experimental conditions were maintained.

Figure 3 shows effect of current on carbon conversion, H_2 yield and gaseous product composition from the anisole steam reforming over NiCuZn-Al_2O_3 catalyst at the temperature range of 500−700 °C. In the case of I=0 (*i.e.*, CSR), the carbon conversion was low (about 24.8%) at 500 °C, and increased to 70.7% at 700 °C. When the current passed through the catalyst (*i.e.*, ECR), the carbon conversion was remarkably enhanced by the current, particularly at low temperature (Fig.3(a)). The carbon conversion increased from 24.8% to 90.8% with increasing the current from 0 to 4 A at the same temperature of 500 °C, and reached nearly complete conversion (99.5%) at 4 A and 600 °C. Figure 3(b) shows dependence of the hydrogen yield on current at given temperature. It was observed that the hydrogen yield was also promoted by the current. The yield of hydrogen was about 17.1% at 500 °C and 0 A, and increased to 67.7% at 500 °C and 4 A. As shown in Fig.3 (c) and (d), hydrogen is the major product with a content of over 60% together with smaller amount by-

DOI:10.1088/1674-0068/23/06/693-700

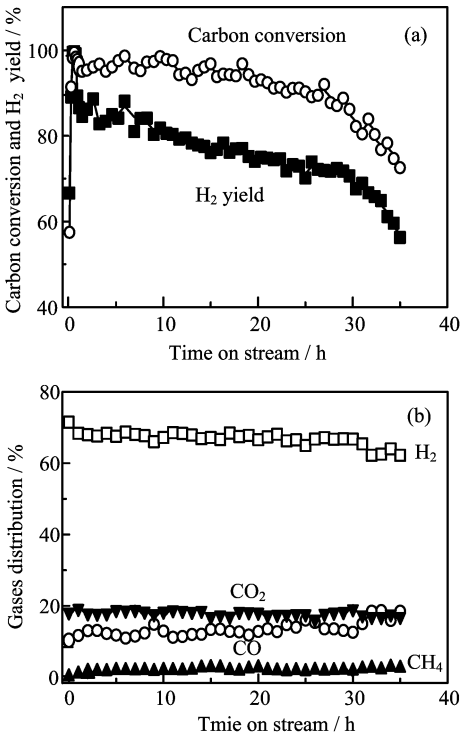

FIG. 4 Stability curves of (a) carbon conversion and H_2 yield (b) gaseous products distribution which were measured under typical ECR reforming of anisole over NiCuZn-Al_2O_3 catalyst. Reforming conditions: T=650°C, I=3 A, f(anisole fed rate)=5.97 g/h, S/C=8, GHSV=2380 h^{-1}, P=101 kPa.

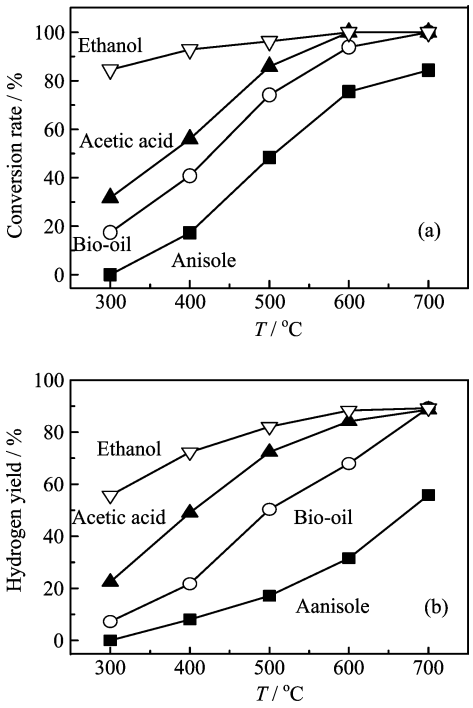

FIG. 5 Conversion rate (a) and H_2 yield (b) for steam reforming of anisole, bio-oil, acetic acid, and ethanol over NiCuZn-Al_2O_3 catalyst. Conditions: T=300−700 °C, S/C=8, GHSV=2380 h^{-1}, $W_{catalyst}$=12 g, P=101 kPa.

products of CO_2 (about 20%) and CO (about 10%). A trace amount of CH_4 (<5%) was also observed in the effluent carbonaceous compounds. It was found that the concentrations of H_2 slightly increased with increasing the current, accompanied by a decrease of the CH_4 concentration. In addition, the stability of the catalyst in the reforming was tested by measuring the carbon conversion, the yield of hydrogen and the gaseous product composition as the function of the time on stream. As shown in Fig.4, no obvious changes in the carbon conversion, the yield of hydrogen, and the product distribution was observed in the initial 10 h. Slow decrease of the carbon conversion and hydrogen yield was found for longer term test, indicating a gradual deactivation of the catalyst during the anisole reforming. The carbon conversion gradually decreases by about 10% (from about 95% to 85%) for 30 h reforming. At the same time, the increase of CO and CH_4 concentration was observed, accompanied by the decrease of H_2 and CO_2 concentration. The catalyst's deactivation, occurring in the process of the anisole reforming, was mainly caused by the carbon deposition on the catalyst.

B. Comparison of different hydrocarbons reforming

As a comparison, the reforming features of ethanol, acetic acid, light fraction of bio-oil (represented as an overall chemical formula of $CH_{2.18}O_{0.6}\cdot 0.77H_2O$) and anisole were investigated over NiCuZn-Al_2O_3 catalyst under the same reforming conditions (Fig.5). Based on the conversion and hydrogen yield, the reforming performance is evaluated, and listed in the following order: ethanol>acetic acid>light fraction of bio-oil>anisole. For example, a nearly complete conversion of ethanol (about 92.9%) can be obtained at 400 °C using the NiCuZnAl catalyst. However, the conversion of the bio-oil and anisole using the same catalyst was very low (about 40.8% and 17.2%) at 400 °C. This should be attributed to different physical and chemical properties and reforming mechanism for different hydrocarbons. Further, the apparent activation energy (E_{app}) of steam reforming is calculated assuming a first order reaction with respect to reactants, as widely accepted in Refs.[26−28]. A major advantage of having a first order reaction is that it is easy for evaluation and comparison with other experiments. The overall rate can be described with the following equation:

$$-r = k_{app}C \tag{6}$$

$$k_{app} = \frac{1}{\tau}[-\ln(1-[A]_{conv})] \tag{7}$$

$$\tau = \frac{W}{v_0} \tag{8}$$

$$k_{app} = A_{app}\exp\frac{-E_{app}}{RT} \tag{9}$$

DOI:10.1088/1674-0068/23/06/693-700

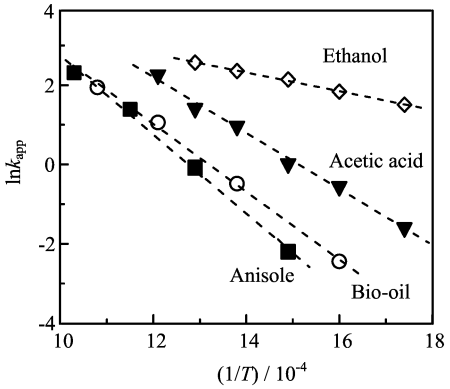

FIG. 6 First-order Arrhenius plots for steam reforming of anisole, bio-oil, acetic acid, and ethanol over NiCuZn-Al_2O_3 catalyst. Conditions: T=300−700 °C, S/C=8, GHSV=2380 h^{-1}, $W_{catalyst}$=12 g, P=101 kPa.

where r is the apparent rate constant, C is concentration of reactant, τ is residual time, A_{app} is apparent preexponential factor, k_{app} is apparent rate constant, W is the mass of catalyst, and v_0 is volumetric flow rate [26−28]. To calculate the activation energy, experiments are performed in the temperature range of 300−700 °C. Temperature dependence on the rate constant (Fig.6) was determined by the Arrhenius equation, from which E_{app} can be calculated. For steam reforming of anisole, bio-oil, acetic acid, and ethanol over NiCuZn-Al_2O_3 catalyst E_{app} are 99.54±4.43, 85.55±3.09, 70.59±2.86, and 23.63±0.67 kJ/mol, respectively. The E_{app} for the steam reforming of anisole is much higher than that of ethanol (23.63 kJ/mol).

It was found that the reforming behavior for the above four samples are quite different, at least in following three respects. Firstly, reforming temperature to achieve an efficient conversion of ethanol for a given catalyst is much lower than that of bio-oil and anisole. For example, a nearly complete conversion of ethanol (about 96.3%) can be obtained at 500 °C, but conversion of bio-oil and anisole were about 74.1% and 48.3% at same temperature using the NiCuZn-Al_2O_3 catalyst. Higher operating temperature for the bio-oil reforming may be due to the fact that the bio-oil contains a large amount of inactive compounds such as phenolics. Secondly, the catalyst deactivation in the anisole and bio-oil reforming, generally, is much more serious than ethanol and acetic acid. The performance of anisole reforming is significantly lower than ethanol, acetic acid, and bio-oil, which should be attributed to the higher stability and strong C−C bond in the phenyl.

C. Decomposition of anisole

The influence of current on the decomposition of anisole was tested via the homogeneous experiments with and without the current. As shown in Fig.7(a), anisole decomposition rate depends on both temperature and the current. Without the current applied, anisole conversion was only 36.0% at 500 °C. However, the rate increased to 73.8% with increasing the current from 0 A to 3 A. It was observed that the hydrogen yield was also enhanced by the current (Fig.7(b)). Figure 8 shows effect of current on the distribution of main gaseous products of anisole decomposition over NiCuZn-Al_2O_3 catalyst at three different temperature of 500, 600, 700 °C. Main gas products from the decomposition of anisole are H_2, CH_4, CO, and CO_2.

Table I shows the selectivity of gaseous and liquid products yielded in anisole decomposition. In addition to the main products from anisole decomposition of H_2, CH_4, CO, and CO_2, the minor components of C_2H_6, C_2H_4, and C_6H_6 were observed. $C_6H_5CH_3$ was also found at low temperature of 500 °C. According to Eq.(17), the majority carbon in anisole finally dehydrogenate into graphite crystallites appearing carbon residue over the catalyst [29, 30].

Anisole decomposition includes complex reaction paths. Based on the previous study, main reaction paths can be described as follows [29−34].

$$C_6H_5OCH_3 \rightarrow C_6H_6 + HCHO \quad (10)$$

$$C_6H_5OCH_3 + HCHO \rightarrow C_6H_5OH + CH_4 + CO \quad (11)$$

$$C_6H_5OCH_3 \rightarrow C_6H_5O + CH_3 \quad (12)$$

$$C_6H_5O \rightarrow 5C + CO + 3H_2 \quad (13)$$

$$CH_3{}^* + H^* \rightarrow CH_4 \quad (14)$$

$$2CH_3{}^* \rightarrow C_2H_6 \quad (15)$$

$$C_6H_5CH_3 \rightarrow C_6H_5{}^* + CH_3{}^* \quad (16)$$

$$C_6H_5OCH_3 \rightarrow 2H_2 + CH_4 + CO + 5C \quad (17)$$

Anisole decomposition into benzene and CH_2O would form in the initial rate-determining step by the intramolecular proton transfer (Eq.(10)), then phenol, methane, and carbon monoxide were successively produced through the fast intermolecular proton and hydride transferring from active formaldehyde to anisole via Eq.(11) [34]. At higher temperature, the formation of C_6H_5O and CH_3 radicals via Eq.(12) was observed to be the principal course of anisole decay [30]. The gas decomposition products of CH_4 and C_2H_6 would be formed according to Eq.(14) and Eq.(15). The effect of current on anisole decomposition appears to promote benzene and toluene decomposition and inhibite Boudouard reaction. Moreover, the existence of current seems favor the production of CH_3 via Eq.(12) at 500 °C, and the decomposition of methane at 600−700 °C.

D. Influence of current on catalyst properties

XRD was employed to investigate the alterations of the NiCuZn-Al_2O_3 catalyst after CSR and ECR of anisole. Figure 9 shows typical XRD spectra for the four different catalyst samples, *i.e.*, the fresh NiCuZn-Al_2O_3 catalyst sample, NiCuZn-Al_2O_3 catalyst sample

DOI:10.1088/1674-0068/23/06/693-700

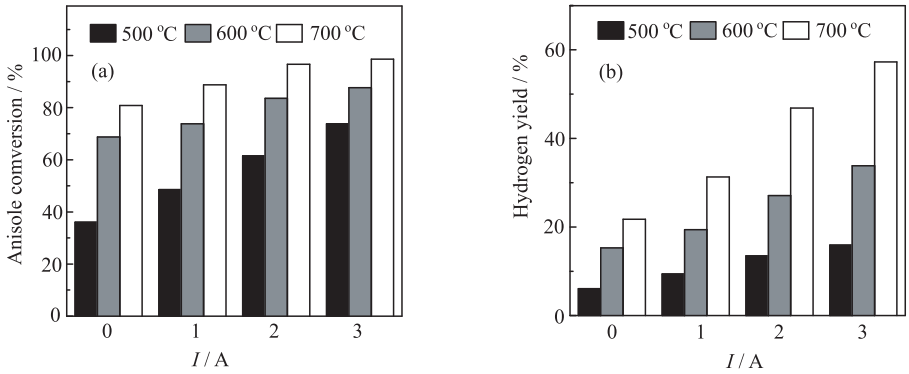

FIG. 7 Effect of current on the anisole conversion (a) and H_2 yield (b) of anisole decomposition over NiCuZn-Al_2O_3 catalyst. Conditions: T=500−700 °C, I=0−3 A, f(anisole fed rate)=5.97 g/h, W_{catalyst}=12 g, P=101 kPa.

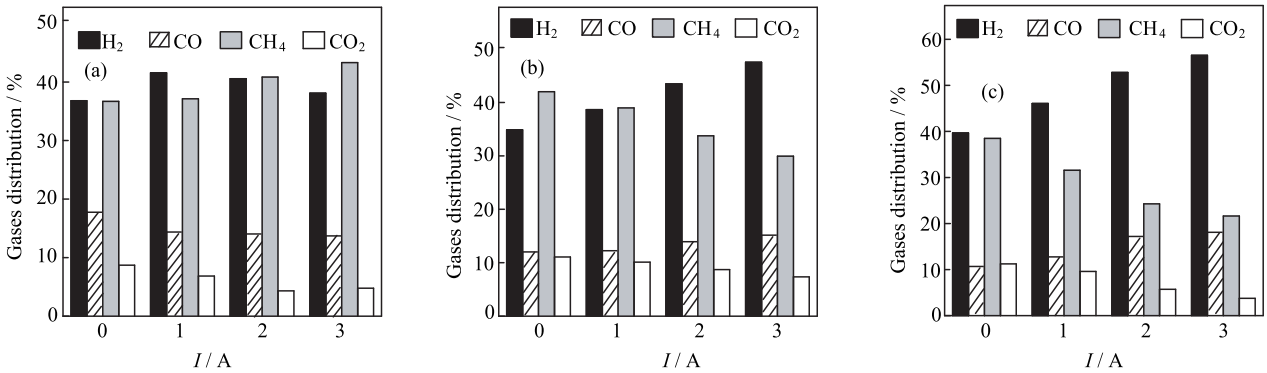

FIG. 8 Effect of current on the distribution of main gaseous products of anisole decomposition over NiCuZn-Al_2O_3 catalyst at different temperatures. Conditions: T=500−700 °C, I=0−3 A, f(anisole fed rate)=5.97 g/h, W_{catalyst}=12 g, P=101 kPa.

TABLE I The selectivity of gaseous and liquid products by anisole decomposition. Conditions: T=500−700 °C, I=0−3 A, f(anisole fed rate)=5.97 g/h, W_{catalyst}=12 g, P=101 kPa.

T/°C	I/A	Gaseous product/%						Liquid product/%	
		H_2	CO	CH_4	CO_2	C_2H_6	C_2H_4	C_6H_6	$C_6H_5CH_3$
500	0	15.37	4.35	9.01	2.13	0.130	0.028	0.069	0.608
	1	18.32	3.72	10.62	1.77	0.072	0.025	0.037	0.337
	2	21.33	4.35	12.63	1.35	0.182	0.068	0.021	0.158
	3	21.53	4.56	14.40	1.60	0.233	0.138	0.007	0.057
600	0	21.65	4.38	15.35	4.04	0.140	0.026	0.200	0
	1	25.58	4.78	15.17	3.94	0.018	0.004	0.162	0
	2	32.38	6.10	14.79	3.81	0.057	0.014	0.112	0
	3	38.58	7.23	14.28	3.53	0.090	0.029	0.032	0
700	0	26.90	4.26	15.35	4.48	0.146	0.036	0.162	0
	1	35.23	5.72	14.19	4.33	0.180	0.066	0.094	0
	2	48.47	9.27	13.09	3.10	0.086	0	0.030	0
	3	58.04	10.95	13.08	2.28	0.003	0	0.016	0

treated by a current of 3 A passing through the catalyst in argon ambience for 8 h, the used NiCuZn-Al_2O_3 catalyst after CSR for 8 h, and the used NiCuZn-Al_2O_3 catalyst after ECR for 8 h, respectively. The existence of NiO phase is confirmed by the diffraction structure at 2θ=37.5°, 43.3°, and 62.9° in the fresh NiCuZn-Al_2O_3 catalyst (Fig.9(a)). The diffraction pattern appeared as three broaden profiles, which indicates NiO is in high dispersive and amorphous state in the fresh catalyst. However, the XRD patterns for the used catalyst after the CSR and ECR reforming are so different that almost all of the NiO phase converted into the metal-

DOI:10.1088/1674-0068/23/06/693-700

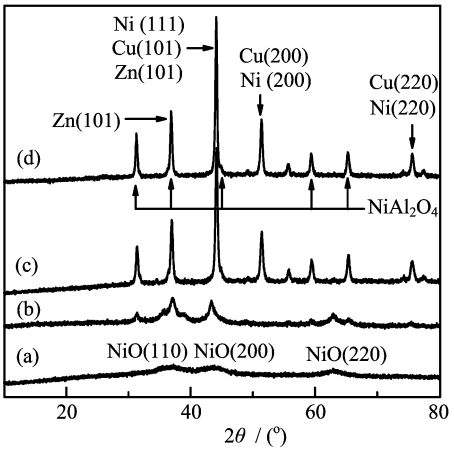

FIG. 9 XRD spectra for (a) fresh NiCuZn-Al_2O_3 catalyst, (b) the NiCuZn-Al_2O_3 catalyst sample treated by a current passing through in argon ambience for 8 h, (c) the used NiCuZn-Al_2O_3 catalyst after CSR for 8 h, and (d) the used NiCuZn-Al_2O_3 catalyst after ECR for 8 h. Conditions: T=600 °C, I=3 A, f(anisole fed rate)=5.97 g/h, S/C=8, GHSV=2380 h^{-1}, P=101 kPa.

lic Ni (*i.e.*, the Ni(111), Ni(200), and Ni(220) peaks at 44.7°, 52.1°, and 76.6°) (Fig.9 (c) and (d)). Especially, the intensity of the diffraction peaks became stronger after the ECR reforming (Fig.9(d)), as comparing with those after the CSR reforming (Fig.9(c)). One of possible explanation is that a part of the oxide states were reduced into the metallic states by the thermal electrons (*i.e.*, $M^{2+}+2e^-\rightarrow M^0$) during the ECR process. Moreover, the NiO reduction was also observed after a current passed through the NiCuZn-Al_2O_3 catalyst in argon ambience, which would be also due to the reduction of the ionic state Ni^{2+} by the thermal electrons. This explanation would be supported by the fact that desorption of thermal electrons from the electrified catalyst was observed by the TOF measurements [16−18].

E. Explanation for the effects of current on the reforming of anisole

Present work shows that the performance of anisole reforming and decomposition are significantly promoted by the current applied during the electrochemical catalytic conversion. Several factors should be considered to account for the current effects observed, as mentioned below. Firstly, it was noticed that the electrochemical catalytic conversion (*i.e.*, inner heating mode) and the conventional catalytic conversion (*i.e.*, outside heating mode) have different temperature distribution in the catalyst bed. The local temperature near the electrified wire was obviously higher than the averaged temperature. Accordingly, the catalyst activity near the electrified wire should be higher than other position in the bed, partly, leading to an increase of the overall catalytic conversion during the electrochemical catalytic conversion process. Secondly, the thermal electrons, originating from the electrified wire, would promote the dissociation of molecular decomposition in the electrochemical catalytic reforming process. The presence of the thermal electrons both on the electrified wire and on the electrified catalyst surface was directly observed by the anionic TOF measurements [16−18]. When an electrified metal or a metal oxide is heated, electrons would boil off its surface, leading to thermal electrons emission from surface [35]. It was reported that thermal electrons on a metal or a metal oxide surface play an important role in the molecular decomposition or ionization processes. Molecular dissociation of O_2, H_2, F_2, H_2O, and hydrocarbons (*e.g.*, benzene, ethanol, HAc) by the thermal electrons was observed in our previous work [36−38]. Accordingly, the thermal electrons may also play a promoting role in the anisole reforming and decomposition during the electrochemical process.

IV. CONCLUSION

The reforming of anisole, which was used as a model compound of the aromatic compounds in bio-oil, was performed by a recently-developed ECR approach over the NiCuZn-Al_2O_3 catalyst. The reforming of anisole was significantly enhanced by the current through the catalyst in the electrochemical catalytic process, which was due to the non-uniform temperature distribution in the catalytic bed and the role of the thermal electrons originating from the electrified wire. The maximum hydrogen yield of 88.7% with a carbon conversion of 98.3% was obtained through the ECR reforming of anisole at 700 °C and 4 A. XRD was employed to characterize the catalyst features and their alterations in the anisole reforming. Based on the conversion rate and hydrogen yield, the reforming performance was evaluated, and listed in the following order: ethanol>acetic acid>light fraction of bio-oil>anisole. The apparent activation energy for the steam reforming of anisole is about 99.54 kJ/mol, which is much higher than ethanol (23.63 kJ/mol) over NiCuZn-Al_2O_3 catalyst. Accordingly, the performance of anisole reforming is significantly lower than ethanol, acetic acid, and bio-oil, which should be attributed to the higher stability and strong C−C bond in the phenyl.

V. ACKNOWLEDGMENTS

This work was supported by the National Natural Science Foundation of China (No.50772107), the National Basic Research Program of Ministry of Science and Technology of China (No.2007CB210206), and the National High Tech Research and Development Program (No.2009AA05Z435).

DOI:10.1088/1674-0068/23/06/693-700

[1] P. D. Vaidya and A. E. Rodrigues, Chem. Eng. J. **117**, 394 (2006).
[2] A. Haryanto, S. Fernando, N. Murali, and S. Adhikari, Energy Fuels **19**, 2098 (2005).
[3] D. Das and T. N. Veziroğlu, Int. J. Hydrogen Energy **26**, 13 (2001).
[4] M. Marquevich, G. W. Sonneman, F. Castells, and D. Montane, Green Chem. **4**, 414 (2002).
[5] J. R. Galdamez, L. Garcia, and R. Bilbao, Energy Fuels **19**, 1133 (2005).
[6] R. C. Saxena, D. Seal, S. Kumar, and H. B. Goyal, Renew Sustain Energy Rev. **12**, 1909 (2008).
[7] S. Rapagnà, N. Jand, and P. U. Foscolo, Int. J. Hydrogen Energy **23**, 551 (1998).
[8] S. Turn, C. Kinoshita, Z. Zhang, D. Ishimura, and J. Zhou, Int. J. Hydrogen Energy **23**, 641 (1998).
[9] P. M. Lv, J. Chang, T. J. Wang, Y. Fu, Y. Chen, and J. X. Zhu, Energy Fuels **18**, 228 (2004).
[10] T. J. Wang, J. Chang, and P. M. Lv, Energy Fuels **19**, 637 (2005).
[11] W. Z. Li, Y. J. Yan, T. C. Li, Z. W. Ren, M. Huang, J. Wang, M. Q. Chen, and Z. C. Tan, Energy Fuels **22**, 1233 (2008).
[12] A. V. Bridgwater, D. Meier, and D. Radlein, Org. Geochem. **30**, 1479 (1999).
[13] A. V. Bridgwater and G. V. C. Peacocke, Renew Sustain Energy Rev. **4**, 1 (2000).
[14] A. V. Bridgwater, Chem. Eng. J. **91**, 87 (2003).
[15] D. Mohan Jr. and C. U. Pittman, Energy Fuels **20**, 848 (2006).
[16] Y. Q. Chen, L. X. Yuan, T. Q. Ye, S. B. Qiu, X. F. Zhu, and Y. Torimoto, Int. J. Hydrogen Energy **34**, 1760 (2009).
[17] L. X. Yuan, T. Q. Ye, F. Y. Gong, Q. X. Guo, Y. Torimoto, and A. Yamamoto, Energy Fuels **23**, 3103 (2009).
[18] Z. X. Wang, Y. Pan, T. Dong, X. F. Zhu, T. Kan, L. X. Yuan, Y. Torimoto, M. Sadakatab, and Q. X. Li, Appl. Catal. A **320**, 24 (2007).
[19] Z. X. Wang, T. Dong, L. X. Yuan, T. Kan, X. F. Zhu, and Y. Torimoto, Energy Fuels **21**, 2421 (2007).
[20] L. X. Yuan, Y. Q. Chen, C. F. Song, T. Q. Ye, Q. X. Guo, and Q. S. Zhu, Chem. Commun. 5215 (2008).
[21] Mi-Kyung Bahng, C Mukarakate, D J. Robichaud, and M R. Nimlo, Analy. Chim. Acta **651**, 117 (2009).
[22] A. V. Friderichsen, Eun-Jae Shin, R. J. Evans, and M. R. Nimlos, Fuel **80**, 1747 (2001).
[23] K. Okuda, S. Ohara, M. Umetsu, S. Takami, and T. Adschiri, Bioresource Technol. **99**, 1846 (2008).
[24] M. H. Waldner and F. Krumeich, J. Supercritical Fluids **43**, 91 (2007).
[25] K. Takanabe, K. Aika, K. Seshan, and L. Lefferts, Chem. Eng. J. **120**, 133 (2006).
[26] L. Devi, K. J. Ptasinski, and F. J. J. G. Janssen, Fuel Pro. Technolo. **86**, 707 (2005).
[27] C. S. Li, D. Hirabayashi, and K. Suzuki, Fuel Pro. Technol. **90**, 790 (2009).
[28] D. Ś wierczyński, S. Libs, C. Courson, and A. Kiennemann, Appl. Catal. B **74**, 211 (2007).
[29] B. E. Koel, J. E. Crowell, B. E. Bent, C. M. Mate, and G. A. Somorjai. J. Phys. Chem. **90**, 2949 (1986).
[30] J. N. Russell, Jr., S. S. Saks, R. E. Morris. Surf. Sci. **338**, 189 (1995).
[31] Isabel W. C. E. Arends, Robert Louw, and Peter Mulder, J. Phys. Chem. **97**, 7914 (1993).
[32] M. Pecullan, K. Brezinsky, and I. Glassman. J. Phys. Chem. A **101**, 3305 (1997).
[33] V. V. Platonov, V. A. Proskuryakov, S. V. Ryl'tsova, and Yu. N. Popova, Rus. J. Appl. Chem. **74**, (2001).
[34] Y. Tsujino, C. Wakai, N. Matubayasi, and M. Nakahara, Chem. Lett. **35**, (2006).
[35] G. A. Somorjai, *Introduction to Surface Chemistry and Catalysis*, New York: Wiley, 362 (1994).
[36] C. F. Song, J. Q. Sun, S. B. Qiu, L. X. Yuan, J. Tu, and Y. Torimoto, Chem. Mater. **20**, 3473 (2008).
[37] F. Huang, J. Li, L. Wang, T. Dong, J. Tu, Y. Torimoto, M. Sadakata, and Q. X. Li, J. Phys. Chem. B **109**, 12032 (2005).
[38] Q. X. Li, K. Hayashi, M. Nishioka, H. Kashiwagi, M. Hirano, Y. Torimoto, H. Hosono, and M. Sadakatad, Appl. Phys. Lett. **80**, 4259 (2002).

DOI:10.1088/1674-0068/23/06/693-700